Electrochemistry Communications 125 (2021) 106985

Contents lists available at ScienceDirect

Electrochemistry Communications

journal homepage: www.elsevier.com/locate/elecom

Full Communication

Electrochemical production of Al–Mn alloys during the electrodeposition of aluminium in a laboratory cell

Omar Awayssa [a,*], Geir Martin Haarberg [a], Rauan Meirbekova [b], Gudrun Saevarsdottir [b]

[a] Department of Materials Science and Engineering, NTNU, Sem Sælands vei 12, Trondheim NO-7491, Norway
[b] Reykjavik University, School of Science and Engineering, Menntavegi 1, 101, Reykjavik, Iceland

ARTICLE INFO

Keywords:
Aluminium
Manganese
Aluminium-manganese alloys
Electrodeposition
Current efficiency

ABSTRACT

This study reports the direct production of an aluminium–manganese alloy during aluminium electrolysis in fluoride-based melts. Experiments were conducted in a laboratory cell dedicated for current efficiency measurements. The temperature was varied from 965–980 °C at a cathodic current density (CCD) of 0.9 A/cm^2 and a cryolite ratio (CR) of 2.2. The manganese content was up to 3.0 wt%. Manganese was added in the form of Mn_2O_3. Bath samples were collected regularly and analyzed with ICP-MS to observe the decay of manganese during electrolysis. It was possible to produce Al-Mn alloys of up to 21 wt. % Mn. Current efficiency for the electrodeposition of Al–Mn alloy was estimated to be in the range of 93%. Current efficiencies with respect to aluminium were estimated. The solidified surfaces of the metal deposits were mostly flat, but some were deformed.

1. Introduction

In the Hall–Héroult process liquid aluminium is produced by the electrolytic reduction of alumina (Al_2O_3) dissolved in an electrolyte containing cryolite (Na_3AlF_6) at 960–970 °C according to the overall electrochemical reaction given by [1]:

$$2Al_2O_3(\text{dissolved}) + 3C(s) = 4Al(l) + 3CO_2\ (g) \quad (1)$$

Manganese is the principal alloying element in the 3xxx aluminium alloys series. A limited percentage of up to 1.5 wt. % Mn added to Al makes the alloy higher in corrosion resistance and much stronger than the commercial pure aluminium. The improvements in the mechanical properties adapts the alloy for the wide use in moderate strength applications requiring good workability [2,3] in various applications. The melting point of manganese is 1245 °C and that of aluminium is 660 °C [4]. The rate of the dissolution of manganese in molten aluminium is very slow which very much depends on the particle size of the added manganese [4]. When manganese in powder form is added to molten aluminium it may float on the surface and forms a hard crust which means some of it may be oxidized [4]. A patent has reported the possibility of producing aluminium–manganese alloys directly in the cryolite-based melt. According to this invention, aluminium–manganese alloys containing up to 10 wt. % Mn have been prepared by adding either MnO, MnO_2, or their mixtures to aluminium in cryolite-based electrolyte [5].

An Al_6Mn phase is likely to form when the content of the manganese is about 14.3 at. % Mn (25.4% wt. % Mn, T ~ 658 °C) whereas $Al_{12}Mn$ is likely to form when the content is about 7.7 at. % Mn (14.5 wt. % Mn, T ~511 °C) [6].

The effect of adding oxides containing manganese; namely MnO, MnO_2, and Mn_2O_3, has been investigated in an industrial Hall–Héroult cell [7]. The study found that manganese ended up in the metal regardless of the initial precursor introduced.

The overall reduction reaction of MnO and MnO_2 in fluoride-based melts containing molten aluminium could be given, in order, as:

$$Mn^{2+} + 2e^- = Mn \quad (2)$$

$$Mn^{4+} + 4e^- = Mn \quad (3)$$

If Mn_2O_3 is used as a manganese precursor, then the overall reduction reaction would proceed according to the following:

$$Mn^{3+} + 3e^- = Mn \quad (4)$$

It may be likely to happen that one electron is transferred in one step at a time at the same potential while two, three, or four electrons are not.

The performance of an electrolytic cell may be judged by current

* Corresponding author.
E-mail address: Omar.r.m.awayseh@ntnu.no (O. Awayssa).

https://doi.org/10.1016/j.elecom.2021.106985
Received 30 November 2020; Received in revised form 8 February 2021; Accepted 16 February 2021
Available online 27 February 2021

efficiency measurements. Current efficiency (CE) is a representation of how efficient the supplied electricity has been used to deposit aluminium. It can be estimated by metal weight gain relating the actual produced aluminium to the aluminium that would theoretically be produced based on Faraday's law. Then CE% may be written as:

$$CE\% = \frac{m_{actual}}{m_{theoretical}} \times 100 = \frac{m_{actual}}{M\ I\ t/zF} \times 100 \quad (5)$$

where m_{actual} is the actual mass of the metal produced whereas $m_{theoretical}$ is the theoretical mass of the metal produced according to Faraday's law. M is the molar mass of aluminum, I is the applied current intensity in A, z is the number of electrons transferred, and F is the Faraday constant 96,487C/mol.

In practice, the amount of aluminium calculated based on Faraday's law can never be obtained. There is always a certain amount of aluminium that dissolves in the electrolyte. As a result, the metal is transported outside the diffusion layer close to the cathode where it gets oxidized by CO_2. CO is released and alumina is produced in the back reaction which can be expressed as:

$$2Al(diss.) + 3CO_2(gordiss.) = Al_2O_3(diss.) + 3CO(g) \quad (6)$$

Dissolved species more noble than aluminum will be reduced at the cathode [8]. The current used to co-deposit such species represents a loss in the current efficiency of the electrolysis process.

The average current efficiency for the alloy can be calculated according to:

$$CE_{alloy}\% = \frac{m_{alloy}}{m_{alloy.theoretical}} \times 100 \quad (7)$$

where m_{alloy} is the total mass of the alloy produced experimentally whereas $m_{alloy.theoretical}$ is the theoretical mass of the produced alloy. The theoretical mass of the produced alloy is given by Faraday's law as:

$$m_{alloy.theoretical} = \frac{M_{alloy} It}{z_{alloy} F} \quad (8)$$

where M_{alloy} is the average molecular mass of the alloy and z_{alloy} is the average charge transferred for the deposition of the alloy. The two quantities may be estimated for the Al–Mn alloy according to the electrochemical equivalent given by:

$$M_{equiv.} = \frac{\left[\frac{M_{Al}}{z_{Al}}\right] \cdot \left[\frac{M_{Mn}}{z_{Mn}}\right]}{\left(x_{Al}\frac{M_{Mn}}{z_{Mn}}\right) + \left(x_{Mn}\frac{M_{Al}}{z_{Al}}\right)} \quad (9)$$

Thus CE% for the alloy can be given by:

$$CE_{alloy}\% = \frac{m_{alloy}}{M_{equiv.}\ It/F} \times 100 \quad (10)$$

where M_{Al}, M_{Mn}, z_{Al}, z_{Mn}, x_{Al}, and x_{Mn} are the molecular masses of Al and Mn, their charges, and their mass fractions respectively.

This work reports a study on the electrochemical deposition of an aluminium–manganese alloy during aluminium reduction in fluoride-based melts in a laboratory cell implementing industrial standards. The effect of the presence of Mn on the current efficiency with respect to Al, the current efficiency for the alloy, and the shape of the surface of the solidified deposit are discussed.

2. Experimental

Experiments were carried out in a laboratory cell originally designed by Solli et al. [9] for current efficiency measurements during electrodeposition. The laboratory cell is schematically illustrated in Fig. 1. A graphite crucible with cylindrical sintered alumina side lining of about 10 cm height containing anode, cathode, and electrolyte was used. The anode is cylindrical with a central vertical hole with a diameter of 16 mm passing through it with an inward inclination angle of 10° as well as horizontal holes of the same diameter of that of the bottom vertical hole penetrating the anode. This design provides good convection within the bath so that gas bubbles from the anode pass through the central vertical hole in the bottom allowing electrolyte to flow up and through the horizontal holes on the sides causing the electrolyte to circulate in a loop. By that, the gas bubbles would have less effect on the diffusion layer and thus the current efficiency would not be significantly affected by increased convection.

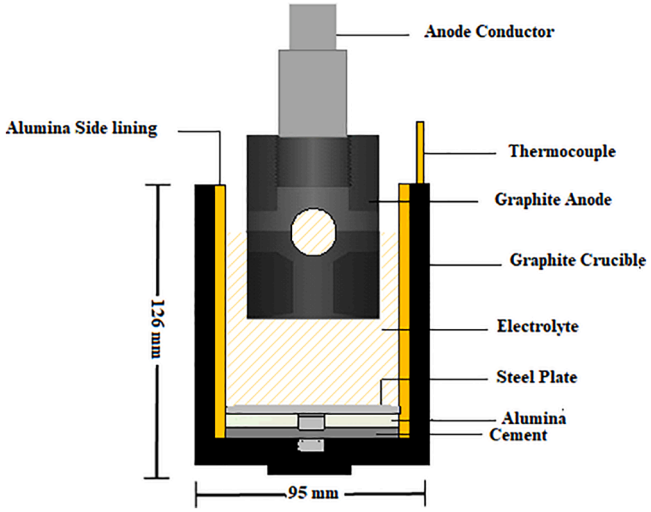

Fig. 1. The design of the electro-deposition laboratory cell used in this work.

The liquid aluminium metal product wets a steel plate resting on the bottom of the graphite crucible and acts as a cathode which ensures an almost flat deposit surface and as a result an even current distribution. A steel pin of 21.0 mm height is placed in a 4.0 mm deep hole at the center of the bottom of the graphite crucible to make a contact with the steel cathode plate. The latter is placed on top of a layer of alumina powder after cementing the bottom of the crucible with a layer of cast alumina cement of 7.0 mm thickness. These two layers should prevent loss of the deposit and minimize chances of aluminium carbide (Al_4C_3) formation. The electrolyte constituents as shown in Table 1 were transferred into the crucible after being dried at 200 °C for 24 hrs. The cell was then placed in a Pythagoras tube inside a vertical furnace. Two copper lids with greased rubber O-rings were used to seal up the two ends of the furnace making it gas-tight. The anode was placed in the bath and held by a steel current collector. The furnace was continuously flushed with argon gas during the experiment in order to prevent air burning of cell components. The temperature was recorded during electrolysis using a thermocouple made of Pt/Pt10Rh placed inside a lateral slot of the crucible.

A DC power supply was used to supply the current. The operating temperature was varied from 965 to 980 °C with a fixed electrolysis duration of 4 h. The corresponding superheat, defined as the difference between the operating temperature and the melt liquidus temperature,

Table 1
Electrolyte constituents.

Chemicals	Pre-treatment	Quality/Supplier
AlF_3	Sublimed at 1090 °C for 24 h	Industrial grade, Alcoa, Norway
NaF	Dried at 200 °C for 24 h	99.5%, Merck, Germany
CaF_2	Dried at 200 °C for 24 h	Precipitated pure, Merck, Germany
Al_2O_3	Dried at 200 °C for 24 h	Anhydrous (γ-alumina), Merck, Germany
Mn_2O_3	Dried at 200 °C for 24 h	325 Mesh powder, 98%, Alfa Aesar, Germany

was varied from 13.0–28.0 °C, being calculated from an equation in [10]. The cathodic current density (CCD) was kept at 0.9 A/cm^2 for all runs. A cryolite ratio (CR) of 2.2 was used for all runs. The standard electrolyte was: 12.0 wt. % AlF_3, 5.0 wt. % CaF_2, 4.0 wt. % Al_2O_3, and balance of NaF–AlF_3 based cryolite. Manganese (III) oxide was initially admixed with the bath constituents prior to electrolysis. Three concentrations were considered based on Mn content: 1 wt. % Mn, 2 wt. % Mn, and 3 wt. % Mn.

The bath was sampled regularly at constant intervals using quartz tubes while keeping the same position of the sampling in the bath for all runs. The collected metal samples were subjected to mechanical and chemical post-treatments, the latter by aluminium chloride hexahydrate solution for 30–40 min. Bath samples were crushed into fine powder and dissolved in a mixture of strong acids including HCl, HNO_3, and HF. The solutions were digested and agitated to ensure a complete dissolution. ICP-MS was conducted for samples afterwards to determine the Mn content in the bath.

3. Results and discussion

3.1. Cell performance

3.1.1. Blank tests

Three blank tests were carried out with no addition of Mn_2O_3 at 965 °C, 970 °C, 975 °C, and 980 °C. Values of current efficiency are shown in Table 2.

Fig. 2 shows the average values of current efficiency at different temperatures. The trendline constructed in Fig. 2 based on the least square regression yielded a reduction in the current efficiency of 0.2% for every 1.0 °C increase in the operating temperature. It agrees with reports which suggest that a reduction in current efficiency of 1% was recorded for every 5 °C increase in the operating temperature [10]. This can be attributed to the fact the increase in the operating temperature would enhance the solubility of the metal into the bath. Blank tests can be considered as benchmarks to check for the effect of the addition of alloying elements on the current efficiency for electrolysis.

3.1.2. Mn addition

Mn_2O_3 was admixed into the bath before melting. Three concentrations were considered: 1.0 wt. % Mn, 2.0 wt. % Mn, and 3.0 wt. % Mn. Temperatures were 965 °C, 970 °C, 975 °C, and 980 °C.

3.1.2.1. Bath analysis. Baths for experiments 1 and 3 mentioned in Table 3 were analyzed for Mn content. As seen in Fig. 4, around 21% of Mn dissolved depleted during the first half of the experiment (120 min) at 965 °C whereas 45% depleted at 980 °C. It is of significance to mention that partial dissolution of Mn_2O_3 in the bath was expected as experiments, in this work, were carried out at saturated (or close to saturation) bath with respect to alumina. Analysis of bath samples taken right before the beginning of electrolysis never yielded the content of Mn initially added as Mn_2O_3.

Table 2
CE of blank tests in Figs. 2 and 3 with some statistical analysis.

Temperature (C)	CE %	CE% mean	Standard deviation (SD)	Standard error (SE)
965	95.8	95.5	0.2	0.1
	95.4			
	95.4			
970	95.1	94.5	0.5	0.3
	94.6			
	93.9			
975	93.8	93.8	0.5	0.3
	94.5			
	93.2			
980	93.8	93.0	0.7	0.4
	93.1			
	92.0			

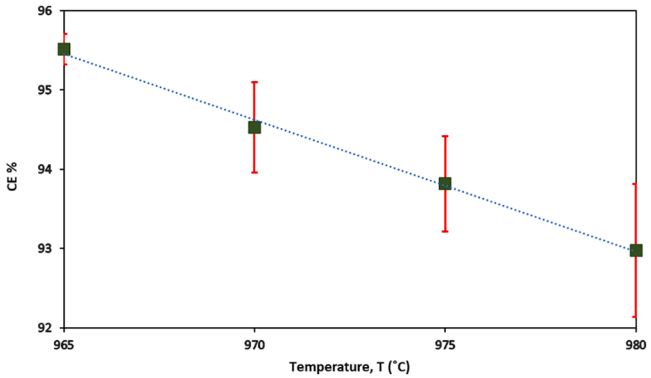

Fig. 2. Average values of CE of blank tests at different temperatures, CR = 2.2, CCD = 0.9 A/cm^2, and electrolysis time 4 h. Error bars are based on the standard error of the mean values from Table 2. The dotted line is based on the least square regression. CE = 256 ± 7.0 – (0.2 ± 0.0) *T*.

3.1.2.2. Solidified deposit analysis. ICP-MS analysis was carried out for the solidified deposits. Table 3 shows the content of Mn in the metal at different temperatures and different initial Mn contents added to the bath. The results suggest that an increase in the content of Mn in the metal was observed upon increasing the initial concentration regardless of the operating temperature. At contents of 1.0 wt. % Mn and 2.0 wt. % Mn initially added to the bath, the final contents of Mn in the metal was around 8.0 wt% and around 13.0 wt. % respectively regardless of the operating temperature which may imply less effect of the latter on the solubility of manganese in the bath. It can also be seen from Table 3 that at a corresponding content of Mn_2O_3 initially added to the bath of 3.0 wt. % Mn, the final contents of Mn in the metal increased upon the increase in the operating temperature. This could be attributed to the enhancement in the solubility of the precursor in the bath which means more Mn is reduced. It also shows that the effect of the operating temperature is more pronounced on the solubility of the oxide than that of the produced metal in the bath.

3.1.3. Current efficiency of Al–Mn alloys

The average current efficiencies of Al–Mn alloys were estimated according to Eqs. (7)–(10). The average current efficiency for the alloy is a representation of the current efficiency of each element based on its content in the alloy. Fig. 4 shows the actual current efficiency for aluminium and the average current efficiency for the aluminium–manganese alloys. Results in the figure mentioned earlier show a difference between CE for Al–Mn alloys and CE for Al of around 4%, 7%, and 9% respectively. The values obtained for Al–Mn current efficiencies were comparable to the blank tests conducted at the same conditions which may indicate the feasibility of the proposed process.

3.1.3.1. Numerical example of calculating current efficiency for Al–Mn alloy. For run 1 from Table 3, the weight of the produced alloy (m_{alloy}) was experimentally found to be 38.81 g. The mass fraction of Mn (x_{Mn}) was determined by ICP-MS for this metallic alloy to be 0.08. Thus, the mass fraction of Al (x_{Al}) is 0.92. The charge transferred during the electrodeposition of Al (z_{Al}) and Mn (z_{Mn}) is 3 equivalent/mol for both. The molar masses of Al (M_{Al}) and Mn (M_{Mn}) are 26.98 g/mol and 54.94 g/mol respectively. Faraday's constant is 96,487 A.s/ equivalent. The

Table 3
Information for actual co-deposition of Mn.

Run #	Temp. (°C)	Initial Mn content added to the bath (wt. %)	Apparent CE% for electrolysis	Conversion % of Mn at actual co-deposition	Deposit Mn content (wt%)	Al–Mn phase likely to form*	Average CE% of Al–Mn	CE% for Al
1	965	1.0	96.8	81.6	8.0	$Al_{12}Mn$	92.9	89.1
2		2.0	98.4	69.1	13.3	$Al_{12}Mn$	91.8	85.4
3		3.0	107.0	56.7	15.0	Al_6Mn	98.8	91.0
4	970	1.0	96.2	78.7	7.7	$Al_{12}Mn$	92.4	88.8
5		2.0	99.9	69.6	13.2	$Al_{12}Mn$	93.2	86.8
6		3.0	101.3	60.5	16.9	Al_6Mn	92.6	84.2
7	975	1.0	92.7	75.9	7.7	$Al_{12}Mn$	89.1	85.5
8		2.0	99.4	70.1	13.3	$Al_{12}Mn$	92.7	86.2
9		3.0	104.5	64.3	17.4	Al_6Mn	95.3	86.3
10	980	1.0	91.3	72.9	7.5	$Al_{12}Mn$	87.8	84.4
11		2.0	100.2	70.5	13.3	$Al_{12}Mn$	93.4	86.9
12		3.0	93.7	68.1	20.6	Al_6Mn	83.8	74.4

*Phases are based on information in [6].

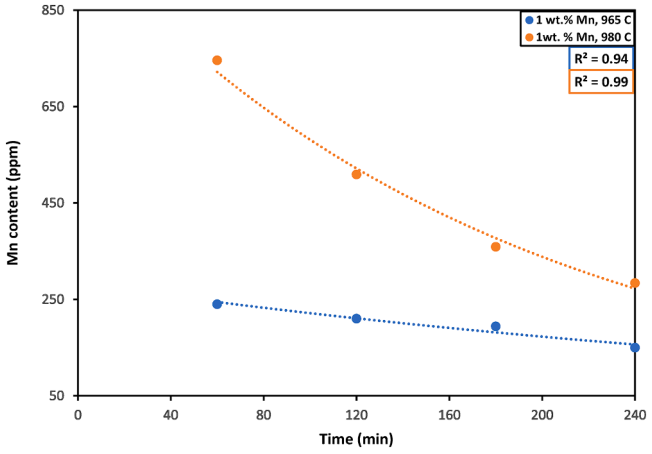

Fig. 3. Decay of Mn in the bath at 1 wt. % content at 965 °C and 980 °C.

current applied to the process, corresponds to 0.9 A/cm^2 current density, is 29.86 A. The electrolysis time is 4 h (14,400 s). Substituting in Eq. (9) gives:

$$M_{\text{equiv.}} = \frac{\left[\frac{54.94}{3}\right] \cdot \left[\frac{26.98}{3}\right]}{\left(0.08 \times \frac{26.98}{3}\right) + \left(\left(1 - 0.08\right) \times \frac{54.94}{3}\right)} = 9.375 \text{g/equivalent}$$

Substituting in Eq. (10) yields:

$$\begin{aligned} \text{CE}_{alloy}\% &= \frac{38.81}{9.375 \times (29.86 \times 14400)/96487} \times 100 \\ &= 92.89 \quad (\textit{rounded to } 92.9) \end{aligned}$$

As seen in Table 3, the content of the co-deposited manganese was in the range of 8–21 wt. %. The ratio of manganese found in the metal to manganese initially added to the bath in the form of Mn_2O_3 is referred to as conversion. Results in Table 3 suggest that around 82% of the 1.0 wt. % Mn initially added to the bath at 965 °C has ended up in the metal. It can also be seen that at 1.0 wt. % Mn initially added a reduction of about 3.0% in the conversion was estimated for every 5 °C increase in the operating temperature. The enhancement in the conversion of Mn was insignificant at 2.0 wt. % Mn and was around 1% at 3.0 wt. % Mn initially added to the bath for every 5 °C increase in the operating temperature.

Apparent current efficiencies of experiments are given in Table 3. Apparent current efficiency here is defined as the ratio percentage of the total weight of the solidified deposit divided by the theoretical mass calculated based on the reduction of aluminium according to Faraday's law. As Mn forms a part of the deposit, the apparent current efficiency can exceed 100%.

Fig. 5 suggests an enhancement of up to 12% in the apparent current efficiency for electrolysis at 965 °C compared to the average CE for Al at the same temperature. An enhancement of up to 7% was estimated for all other temperatures. The enhancement is defined as the difference between the apparent current efficiency at a certain temperature and the average current efficiency for Al at the same temperature.

3.1.4. *Current efficiency for Al*

Blank tests would be a good reference when looking at the effect of the presence of Mn in the deposit on CE. Current efficiency for Al is based on the net weight of Al exists in the solidified deposit. That implies the deduction of the weight of the co-deposited manganese from the total weight of the deposit after cleaning.

Fig. 6 shows a summary of the actual current efficiencies for all temperatures at different initial Mn contents added to the bath. The maximum current efficiency obtained for Al in the alloy was 91.0% at 965 °C and 3.0 wt. % Mn initially added to the bath while the lowest was 74.0% at the same Mn concentration but at 980 °C. A reduction in the CE for Al, with respect to the average current efficiency for Al at the corresponding blank tests, due to the co-deposition of manganese was estimated to be in the range of 5–19% at different conditions as suggested by Fig. 6.

3.2. *Solidified deposit shape and cell voltage behavior*

The solidified deposits' surfaces of all blank tests were flat. Samples of experiments carried out at 965 °C and 980 °C are shown in Fig. 7 indicating even current distributions. Fig. 8 illustrates similar and stable cell voltage behavior of the blank tests with minimum fluctuations.

The solidified deposits' surfaces were flat when experiments were carried out under the addition of 1 wt. % Mn at 965 °C, 970 °C, 975 °C, and 980 °C. A similar cell voltage behavior with drops of at least 600 mV

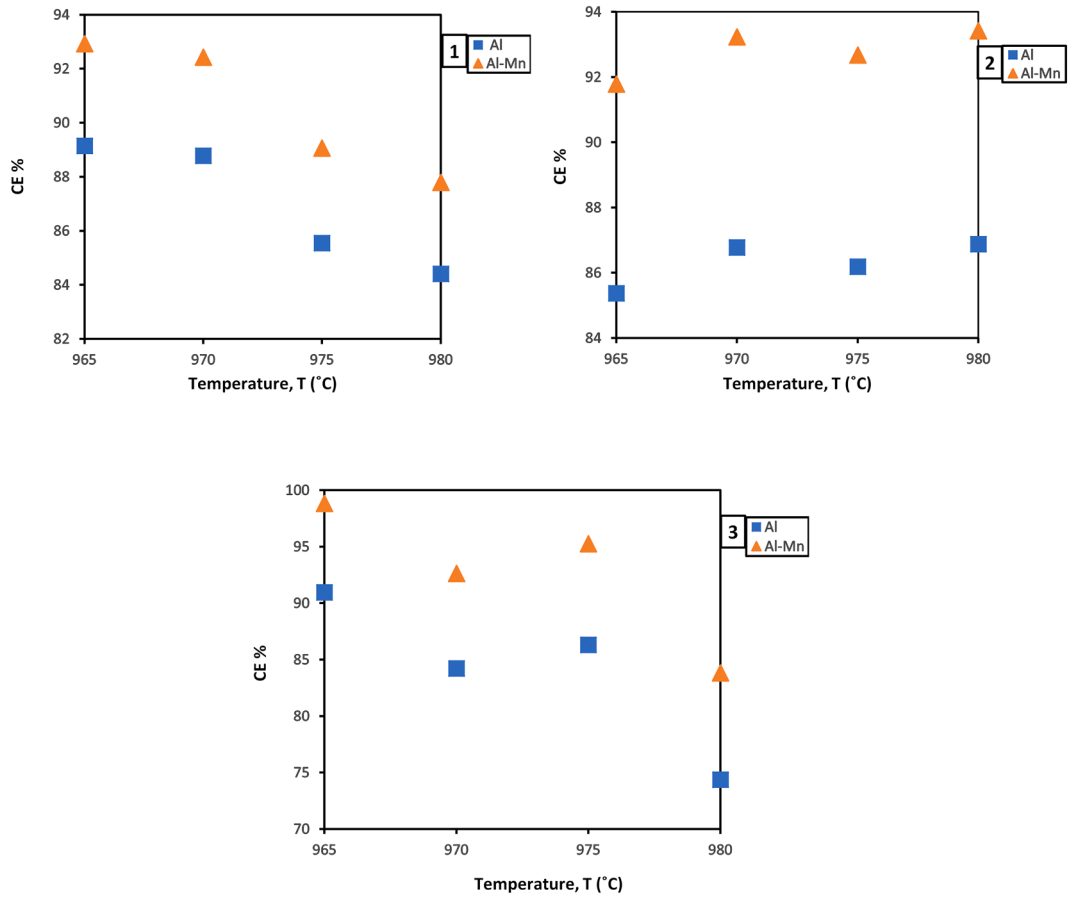

Fig. 4. Actual CE% for Al and average CE% for Al–Mn at initial added Mn of: 1) 1 wt. %, 2) 2.0 wt. %, 3) 3.0 wt. %.

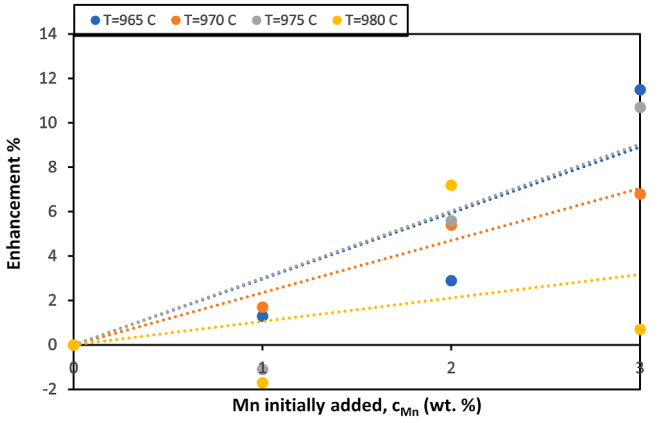

Fig. 5. Enhancement in the apparent CE for electrolysis at different contents of Mn initially added compared to the average current efficiency for aluminium of blank tests. At 965 °C: Enhancement % = (3.0 ± 1.0) c_{Mn}. At 970 °C: Enhancement % = (2.4 ± 0.3) c_{Mn}. At 975 °C: Enhancement % = (3.0 ± 0.9) c_{Mn}. At 980 °C: Enhancement % = (1.1 ± 0.2) c_{Mn}. Intercepts forced to zero.

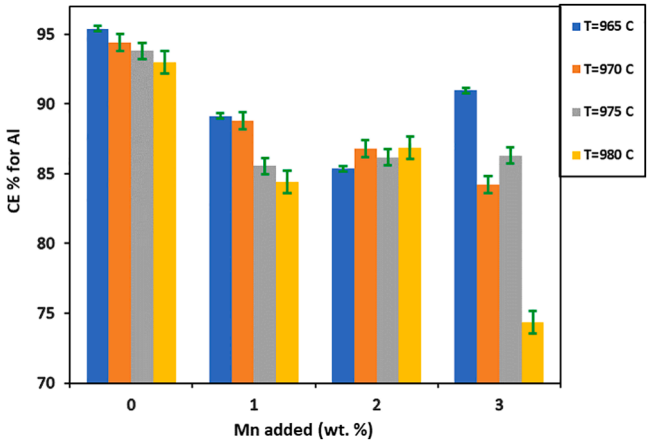

Fig. 6. Summary of actual CE% for Al at different temperatures and Mn contents initially added to the bath.

in the first hour of electrolysis at 965 °C and 970 °C is observed. The cell voltage stabilizes at around 3.9 V for the rest of electrolysis. The cell voltage at 975 °C showed as similar behavior to that at 965 °C and 970 °C but stabilizes around 4.3 V after the first hour of electrolysis. At 980 °C the cell voltage behavior had some fluctuations and did not stabilize but rather steadily increased up to 4.4 V by the end of electrolysis as illustrated in Fig. 9. Such behavior looks somehow similar to that in the blank tests conducted at the same conditions except for the

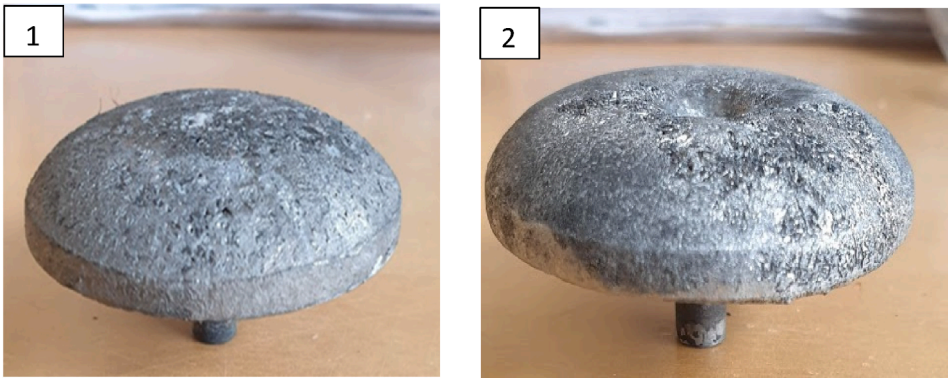

Fig. 7. Blank tests using NaF–AlF_3 cryolite at CR = 2.2, CCD = 0.9 A/cm^2, t = 4 h: 1) (left) T = 965 °C; 2) (right) T = 980 °C.

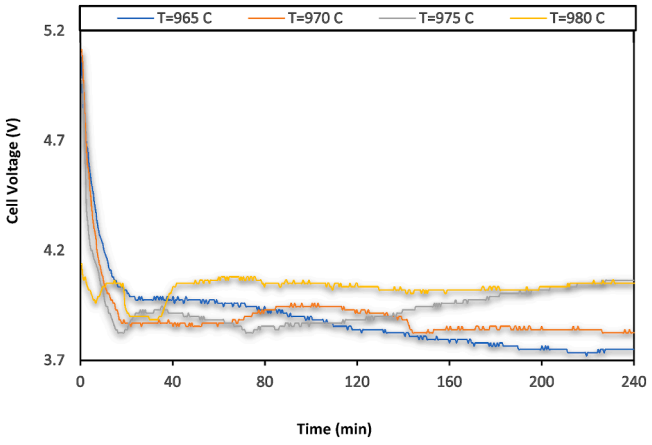

Fig. 8. Cell voltage behavior of blank tests at using NaF–AlF_3 cryolite, CR = 2.2, CCD = 0.9 A/cm^2 at different temperatures.

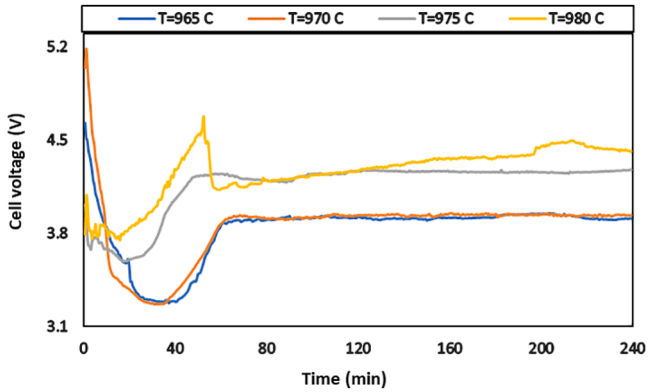

Fig. 9. Cell voltage behavior at initial Mn content of 1.0 wt. % at different temperatures using NaF–AlF_3 cryolite, CR = 2.2, CCD = 0.9 A/cm^2.

significant drops which may be attributed to the co-deposition of Mn.

The solidified deposits' surfaces were mostly flat when experiments were carried out under the addition of 2 wt. % Mn at 965 °C, 970 °C, 975 °C, and 980 °C.

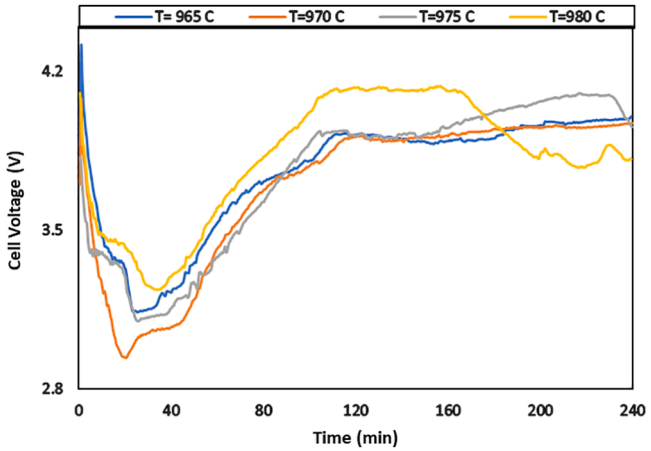

Fig. 10. Cell voltage behavior at initial Mn content of 2.0 wt. % at different temperatures using NaF–AlF_3 cryolite, CR = 2.2, CCD = 0.9 A/cm^2.

A similar cell voltage behavior with drops of at least 600 mV in the first hour of electrolysis at 965 °C and 970 °C is observed. The cell voltage stabilizes at around 3.9 V for the rest of electrolysis. The cell voltage at 975 °C shows a similar behavior to that at 965 °C and 970 °C but stabilizes around 4.0 V after the second hour of electrolysis. At 980 °C the cell voltage behavior has some fluctuations and does not stabilize but rather steadily increases up to 4.2 V and decreases by the end of electrolysis to 3.8 V as illustrated in Fig. 10. As the content of Mn added increased to 2 wt. %, the drops in the cell voltage were higher than that of 1 wt. % in comparison to the cell voltage behavior of the blank tests.

The solidified deposits' surfaces of runs 3 and 9 mentioned in Table 3 were flat as seen in Figs. 11 and 12 (Figure 11.1 and Figure 12.1). However, the deposits' surfaces of runs 6 and 12 in Table 3 were deformed as seen in Figs. 11 and 12 (Figure 11.2 and Figure 12.2). Fig. 13 shows the cell voltage behavior of runs mentioned earlier. A similar cell voltage behavior with drops of at least 1.0 V in the first hour of electrolysis at all temperatures as seen in Fig. 13. The relatively high drops may be due to the relatively high content of Mn (III) which was reduced as there was 3 wt. % Mn initially added as Mn_2O_3.

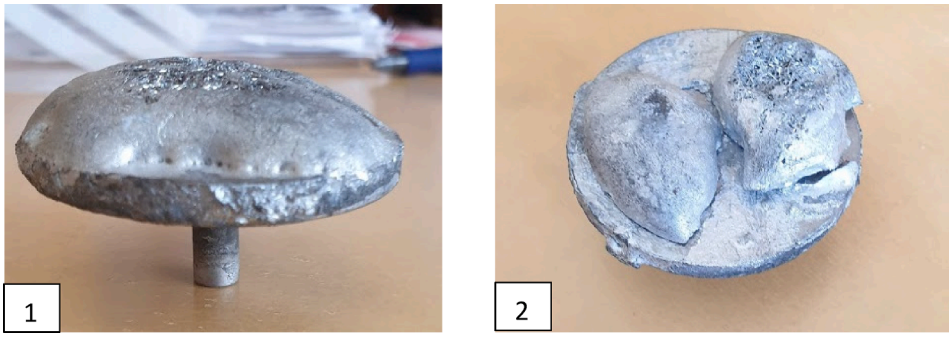

Fig. 11. Deposits using NaF–AlF_3 cryolite at 3 wt. % Mn, CR = 2.2, CCD = 0.9 A/cm^2, t = 4 h: 1) T = 965 °C; 2) T = 970 °C.

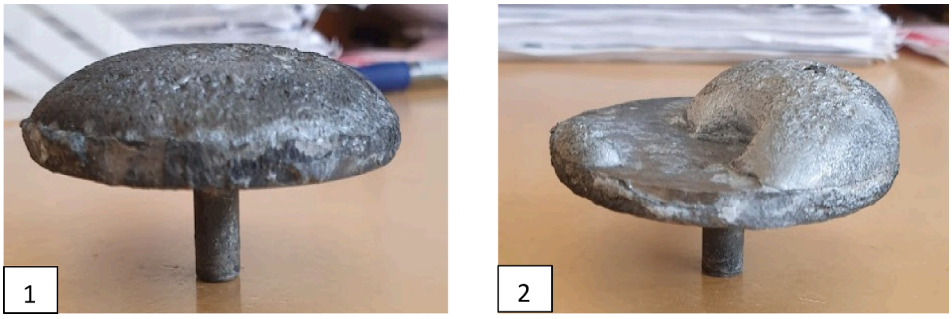

Fig. 12. Deposits using NaF–AlF_3 cryolite at 3 wt. % Mn, CR = 2.2, CCD = 0.9 A/cm^2, t = 4 h: 1) T = 975 °C; 2) T = 980 °C.

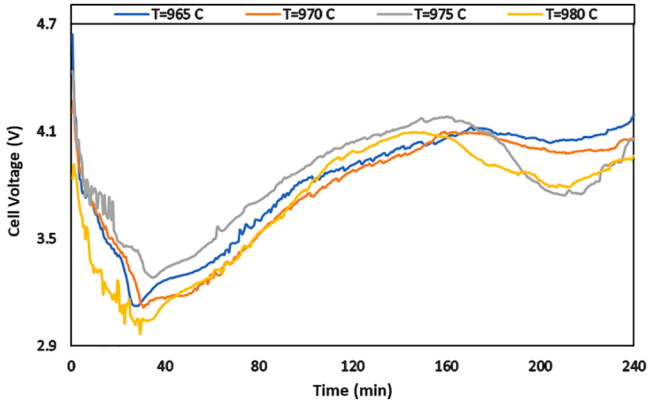

Fig. 13. Cell voltage behavior at initial Mn content of 3.0 wt. % at different temperatures using NaF–AlF_3 cryolite, CR = 2.2, CCD = 0.9 A/cm^2.

4. Conclusions

Experiments of blank tests showed an enhancement of 1% in current efficiency for aluminium deposition when the operating temperature was lowered by 5 °C due to the decrease in the solubility of metal in the bath which agrees with the literature data.

Co-deposition of manganese to produce Al–Mn alloys was studied in a laboratory cell optimized for aluminium current efficiency measurements. Results from ICP-MS suggest that an increase in the content of Mn in the metal upon increasing the initial concentration of added manganese oxide to the bath regardless of the operating temperature. At contents of 1.0 wt. % Mn and 2.0 wt. % Mn initially added to the bath, the final contents of Mn in the alloy was around 8 wt. % and around 13 wt. % respectively regardless of the operating temperature which may imply less effect of the latter on the solubility of manganese (III) oxide in the bath.

The average current efficiencies for Al–Mn alloys have a difference of up to 9% in comparison to those estimated for the actual deposition of Al which implies that this path is quite efficient to produce such alloys. At relatively low initial concentrations of Mn added to the bath at 965 °C around 80% has ended up in the alloy. It can also be seen that at 1.0 wt. % Mn initially added a reduction of about 3.0% in the conversion was estimated for every 5 °C increase in the operating temperature. The enhancement in the conversion of Mn was insignificant at 2.0 wt. % Mn and was around 1% at 3.0 wt. % Mn initially added to the bath for every 5C increase in the operating temperature.

The current is believed to be evenly distributed on the flat surfaces of the blank tests' electrodeposits. Minimum cell voltage fluctuations were observed for such tests. The co-deposition of Mn did not affect the solidified deposits surface shape for most of the runs at different Mn contents and operating temperatures. At high Mn_2O_3 content corresponds to 3.0 wt. % Mn initially added to the bath at 970 °C and 980 °C the deposits' surfaces were deformed.

CRediT authorship contribution statement

Omar Awayssa: Methodology, Investigation, Validation, Writing - original draft. **Geir Martin Haarberg:** Conceptualization, Supervision, Writing - review & editing, Project administration. **Rauan Meirbekova:** Supervision, Writing - review & editing. **Gudrun Saevarsdottir:** Supervision, Writing - review & editing.

Declaration of Competing Interest

The authors declare that they have no known competing financial interests or personal relationships that could have appeared to influence the work reported in this paper.

Acknowledgment

The financial support from the Norwegian University of Science and Technology (NTNU) is greatly acknowledged.

References

[1] K. Grjotheim, H. Kvande, Introduction to Aluminium Electrolysis: Understanding the Hall−Héroult Process, second ed., Aluminium-Verlag, Düsseldorf, 1993.

[2] J. Davis (Ed.), Alloying: Understanding the Basics, first ed., ASM International, Ohio, 2001.

[3] J. Davis (Ed.), Metals Handbook Desk Edition, second ed., ASM International, Ohio, 1998.

[4] J. Kline, W. Yeh, U. Preston, Method of adding manganese to aluminium, USA Patent No.3,865,583, 11 February 1975.

[5] W. King, Aluminium−Manganese Alloy,USA Patent No. 3,951,764, 20 April 1976.

[6] M. Asgar-Khan, M. Medraj, Thermodynamic description of the Mg–Mn, Al–Mn and Mg–Al–Mn systems using the modified quasichemical model for the liquid phases, Mater. Trans. 50 (5) (2009) 1113–1122, https://doi.org/10.2320/matertrans.MRA2008484.

[7] G.M. Haarberg, P. Cui, Mass transfer reactions near the cathode during aluminium electrolysis, Light Metals (2014) 749–752, https://doi.org/10.1007/978-3-319-48144-9_126.

[8] K. Grjotheim, K. Matiasovsky, Impurities in the aluminium electrolyte, Aluminium 59 (1983) 687.

[9] P. Solli, T. Eggen, S. Rolseth, E. Skybakmoen, Design and performance of a laboratory cell for determination of current efficiency in the electrowinning of aluminium, J. Appl. Electrochem. 26 (10) (1996), https://doi.org/10.1007/BF00242196.

[10] A. Solheim, S. Rolseth, E. Skybakmoen, L. Støen, Å. Sterten, T. Støre, Liquidus temperatures for primary crystallization of cryolite in molten salt systems of interest for aluminum electrolysis, Metall. Mater. Trans. B. 27B (1996) 739–744, https://doi.org/10.1007/BF02915602.